Intermetallic compounds of the Cr–Mn system investigated using in situ powder neutron diffraction: The reported order-disorder transformation of the σ phase elucidated

Jean-Marc Joubert

Intermetallic compounds of the Cr–Mn system investigated using *in situ* powder neutron diffraction: the reported order-disorder transformation of the σ phase elucidated

Jean-Marc Joubert
Univ Paris Est Creteil, CNRS, ICMPE, UMR 7182, 2 rue Henri Dunant, 94320 Thiais, France
jean-marc.joubert@cnrs.fr

Keywords
Cr–Mn; phase diagram; neutron diffraction; σ phase; order-disorder

Abstract

Cr–Mn system is very important for many applications. In the present work, the reported intermetallic compounds have been studied using *in situ* high temperature neutron powder diffraction. For the first time, site occupancies in a σ phase are obtained as a function of temperature by Rietveld analysis. They are compared with calculated data obtained from DFT. The previously reported order-disorder transition in the σ phase around 1000°C is shown to be in fact a congruent phase transformation to the *bcc* Cr–Mn solid solution. This solid solution is probably continuous between pure Cr and δ-Mn. The second reported intermetallic α' phase (Cr_2Mn_3) phase is shown to be in fact a ternary nitride of the Cr–Mn–N system that should not appear in the binary phase diagram. The present work clarifies and explains all the features of the previous literature on this system and brings major revisions to the phase diagram. General conclusions are drawn concerning mistakes that can be done in the evaluations of phase diagrams.

1. Introduction

The constitution of Cr–Mn system is obviously very important for many different applications, among which steel because both chromium and manganese are very important alloying elements. This system is characterized by the occurrence of the σ phase that deserves a particular attention. Due to its brittleness, it should be absolutely avoided in commercial alloys. It is a Frank-Kasper phase, common in many other transition metal systems, containing 5 sites in the space group $P4_2/mnm$ [1]. It is characterized by a high degree of non-stoichiometry accommodated by atom mixing on the different sites. As it also exists in Cr–Fe system, its stability in Cr–Mn system and its extension into the ternary Cr–Fe–Mn system should be considered of prime interest in the frame of steel application. However, its stability in Cr–Mn system is still matter of great uncertainty. There are reports by different experimental techniques (differential thermal analysis, magnetic susceptibility, thermal expansion) of a phase transition as a function of temperature. The transition is represented in the phase diagram of Fig. 1. In order to elucidate the nature of the transition(s) reported in the phase diagram, we performed *in situ* powder neutron diffraction (ND) experiments as a function of temperature. This type of measurement also allows the determination of site occupancies as a function of temperature. Such a determination for the σ phase in any system is missing in the literature.

2. Literature survey

2.1. Presentation

2.1.1. The σ phase

The Cr–Mn system has been entirely reviewed and evaluated by Venkatraman and Neumann [2]. The occurrence of an intermediate phase in this system has been shown independently by Carlile *et al.* [3] and Zwicker [4]. The crystal structure was later recognized as that of the σ phase [5]. The possibility of a phase transition has been first proposed by Zwicker [6]. This proposal has been made upon the presence of a thermal arrest and a large jump in the thermal expansion around 975°C. Pearson and Hume-Rothery confirmed this behavior [7] also by thermal analysis. They noted that samples quenched from temperatures above and below the transition have the same X-ray diffraction (XRD) crystal structure. Additionally, *in situ* XRD measurements above the transition temperature were conducted which also failed to detect a difference between the high and low temperature XRD patterns. It was proposed that the transition could be an order-disorder transition. The absence of any related change of the XRD pattern is explained by the fact that changes of the site occupancies cannot be detected because of the lack of diffraction contrast between the two atoms. A significantly new contribution to the work was brought by Wachtel and Bartelt [8] using conventional characterization of different alloys and particularly detailed analysis of the magnetic susceptibility function of temperature and composition. They confirmed the presence of a transition around 1000°C and they even found a second transition at 800°C. The jump in thermal expansion was also confirmed by Gerspacher [9].

By ultra-fast quenching from the melt, Gudzenko and Polesya obtained the *bcc* phase in the composition region where the σ phase should form [10, 11]. This phase in this region was thought to be metastable.

Contrary to XRD, ND is very sensitive to the level of ordering between Cr (b_{Cr}=3.6 fm) and Mn (b_{Mn}=-3.7 fm) because the diffraction contrast is huge. Algie and Hall performed a ND experiment on a sample quenched from the

melt [12]. Kasper and Watestrat obtained ND patterns of samples quenched from 1100°C and 850°C [13] without showing clear qualitative differences due to the poor quality of the diffraction patterns. At this step, one should mention that, while the diffraction contrast between the two elements is very favorable to the determination of site occupancies, the cancelling effect of the scattering factors (Fermi lengths are of opposite signs) when the atoms mix produces very low diffraction intensities. More recently, a similar experiment was repeated with samples quenched from the high (1100°C) and the low (900°C) temperature regions. This time, precise quantitative site occupancies were obtained from a Rietveld refinement and did not show any sign of disordering since the refined site occupancies were almost similar [1].

2.1.2 The α' (Cr_2Mn_3) phase

Pearson *et al.* [7] first noticed the possible occurrence of a second intermediate compound in the system at a composition close to 60 at.% Mn. It was always observed as a third phase in alloys with *bcc* and σ and the conditions for its formation were not clearly established. It is thought to decompose peritectoidally at 600°C. The structure was identified as similar to that of αMn. The occurrence of this phase was confirmed by Wachtel and Bartelt [8] but with a much higher temperature stability up to 925°C and an order-disorder transition at 600°C. The presence of only one diffraction line corresponding to αMn was also confirmed.

2.1.3. Sensitivity to nitrogen

Already in the first studies of this system, the extreme sensitivity of Cr–Mn alloys to nitrogen was noticed [3, 6, 14]. When annealing treatment is performed above 1050°C or 1100°C, it seems that quartz tubes are permeable enough to nitrogen and alloys are so sensitive that nitrides can be formed. This feature was also confirmed by Wachtel and Bartelt [8]. Studies of the Cr–Mn–N system are available in the literature [15, 16].

2.2 Preliminary conclusions

Order-disorder transitions involving the σ-phase have been hypothesized in quite a few binary systems. They have been reviewed in Ref. [1]. Though it is proved that transitions exist in these systems, the nature of the transition itself has never been identified from a structural point of view in any system. So, it is time to check this with adequate structural tools.

In the case of Cr–Mn system, the presence of a clear thermal arrest and a huge jump of the thermal expansion, corroborated by magnetic susceptibility changes, at around 1000°C is in favor of a first-order phase transition. As alloys quenched from the high and low temperature fields both give the same XRD pattern of the σ phase, the transformation is supposed to be an order-disorder phase transition keeping the average structure of the σ phase. From XRD, Cr and Mn cannot be distinguished. This means that one can neither prove nor disprove the ordering or disordering between the two elements. However, room temperature ND of the same type of samples, despite the excellent contrast between elements, could not show a difference of the state of order.

The presence of an order-disorder transition is rather unlikely since the σ phase is very prone to have a substitutional disorder to accommodate the departure from the ideal stoichiometry (Cr_2Mn in our case, very far from the composition at which it is observed). If ND measurements are characteristic of the low temperature state, then, already at low temperature, the amount of disorder is very large, and it is difficult to imagine that a more disordered state would necessitate a first-order phase transition with significant heat of transformation and a huge jump of thermal expansion. It is even more difficult to imagine that two different order-disorder transitions are present as suggested by Wachtel and Bartelt [8].

To summarize, all the techniques used up to now to study the phase transition in the σ phase are indirect techniques. They show a transition at ~1000°C but do not demonstrate the structural nature of the transition. Our structural *ex situ* ND measurement was in contradiction with the existence of a transition. The only possibility to reconcile all the experiments is to suppose that the high temperature phase, whatever it is, cannot be retained by quenching. It should therefore be studied *in situ* and ND is necessary to examine the state of order. The present work is therefore reporting new *in situ* ND experiments that have been carried out as a function of temperature for two σ phase samples.

3. Experimental details

Two samples ($Cr_{21}Mn_{79}$ and $Cr_{23}Mn_{77}$) have been synthesized by induction melting of the pure components followed by two annealing treatments: one at high temperature (1100°C, one week) to homogenize the samples, one at low temperature (700°C, three weeks) to equilibrate the samples in the low temperature phase field. The samples were characterized by conventional techniques: electron probe micro-analysis (EPMA, CAMECA SX100) and XRD. The samples (around 7 g) were reduced into powder (<63 µm). The powder ND experiment was performed at the ILL on D1B instrument (λ=1.29 Å, 2θ range 1-129°). The powders were contained in a Nb can, fitted in the high-temperature furnace under vacuum. Temperature scans were programmed from room temperature up to 1200°C (heating and

cooling) and the diffraction was measured as a function of temperature continuously in different temperature scans. Phases were identified and the ND patterns were refined using the Rietveld method. This includes an accurate site occupancy refinement when the σ phase is present with composition constraint as explained in Ref. [1] following the method developed in Ref. [17]. Additionally, a sample of composition $Cr_{34}Mn_{66}$ was also synthesized and subjected to different annealing treatments. For this sample, XRD and EPMA characterization but not ND were performed. Additional EDS and EBSD characterization was obtained using a Carl Zeiss-Merlin scanning electron microscope.

4. Results

The main finding of the present work is the identification of the transition occurring around 1000°C. The results show that it is not an order-disorder transition within the σ phase like previously proposed but rather a phase transition from σ to a *bcc* disordered solid solution. The transformation cannot be retained by quenching *i.e.* the *bcc* phase transforms back to the σ phase whatever the cooling rate operated during the *in situ* experiment. This explains why this transformation could not be identified in previous work.

4.1. $Cr_{21}Mn_{79}$

During the preliminary characterization by EPMA and XRD, this sample was found to be single phase (see Table S1 in Supplementary Material). The ND analysis at room temperature shows the presence of MnO phase (Fig. 2). Though it is present in a very small amount (less than 1 wt.%), it is clearly seen in all the diffraction patterns because ND is very sensitive to the presence of this phase. During the experiment and excursion at high temperature, the amount will not increase testifying the quality of the atmosphere during the measurement.

In the ND experiment, the sample was first measured at room temperature in a vanadium container, then placed in a niobium can for the high temperature measurement. Heating was done from 550°C to 1200° by step of 50°C (see the timeline in Fig. S1 of the Supplementary Material, the detailed ND results are gathered in an Excel sheet in Supplementary Material). After temperature (fast) stabilization at each step, a 30 min diffraction pattern was measured. Between 1000°C and 1050°C, the σ phase is completely transformed into a disordered *bcc* phase (see Fig. 3).

After heating up to 1200°C, the temperature was then decreased with smaller temperature steps (10°C, the reverse transformation is observed between 1010°C and 990°C), then with 50°C steps down to 550°C. The sample was heated again and the transformation to the *bcc* phase is observed again between 1010°C and 1030°C showing a perfect reversibility and reproducibility. Finally, the sample was quenched by turning off the furnace allowing a rather rapid cooling (40°C/min). During the cooling, the patterns were recorded at first during 1 min then 5 min. Rapid transformation into the σ phase is observed showing that it cannot be quenched in these conditions.

During the analysis using the Rietveld method, lattice parameters of the MnO, Nb, σ and *bcc* have been followed, as well as displacement parameters, phase amount and site occupancies in the σ phase (internal parameters have been kept fixed). All the results are available in Supplementary Material.

During the first cooling done at moderate cooling rates, strange diffraction intensities are observed for the σ phase. Though the peaks of the σ phase can be all indexed in the structure, a good fit of the intensities can no longer be obtained. As a matter of fact, the intensities not only cannot be described by letting free the site occupancies and internal parameters, but also vary erratically from a diffraction pattern to another. It is found after the experiment that the powder sample has sintered. Post-mortem XRD powder diffraction on a slice of the sintered sample shows a heavily textured material while if the sample is reduced into powder the normal structure of the σ phase is obtained. The anomalies are therefore explained by a texture caused by a very large grain growth during the excursion at high temperature, the transformation from single phase *bcc* to σ and the slow cooling rate that has been applied at the first cooling cycle. Additionally, EBSD measurements were performed and confirm the large grain growth of the sample with grains reaching millimeter size (see Fig. S2 in Supplementary Material) impeding a statistical orientation of the grains in the beam and the acquisition of correct intensities. The consequence is that site occupancies can no longer be refined in the ND patterns.

4.2. $Cr_{23}Mn_{77}$

The main difference with the first sample, apart from different nominal and analyzed compositions, is the presence of an additional phase. The second phase is identified as being a nitride by EDX analysis showing an approximate concentration of nitrogen of 20 at.%. From XRD, a *fcc* phase can be identified. The presence of αMn phase is also noticed (see the complete characterization in Table S1 of Supplementary Material).

From ND pattern taken at room temperature, it is evident that the structure of the second phase is not a disordered *fcc* but rather a $L1_2$-derived phase (see the comparison in Fig. 4). It is not possible to see the ordering between Cr and Mn with XRD so that only the lines with *h*, *k* and *l* having the same parity are visible (111 and 200). On the contrary, superstructure peaks (100, 110, 210, 211) have a very large intensity in the ND pattern due to the opposite values of b_{Cr} and b_{Mn}.

The phase is a substitutional derivative of Mn_4N phase already studied by Juza *et al.* [15]. These authors proposed a structure model that could be refined in the present work including the distribution of the metallic elements and the amount of interstitial nitrogen (see the complete results in Supplementary Material).

Measurements have been done during heating, see the timeline in Fig. S3 of Supplementary Material. Between 600°C and 900°C, the αMn phase disappears and the ordered nitride is shown to disorder. All the superstructure peaks of the filled $L1_2$ disappear and a *fcc* phase is refined with interstitial N (see Fig. S4 in Supplementary Material). The transition is accompanied by a significant decrease (1.4%) of the lattice parameter (probably related to the loss of nitrogen accompanying the transition). At higher temperature, the nitrogen content decreases in particular when the σ phase is transformed into *bcc*. Probably, nitrogen dissolves into the *bcc* phase. At even higher temperature, the *fcc* nitride eventually disappears completely.

As in sample $Cr_{21}Mn_{79}$, site occupancies were obtained as a function of temperature. The transformation of the σ phase into a *bcc* phase is also observed. The transition temperature is slightly lower. At 960°, there seems to be a coexistence between the two phases while at 980°C, the σ phase has completely transformed.

The sample was heated up to 1040°C. Due to a technical problem, while cooling, the sample was held at 1020°C for three hours without acquisition. It was finally quenched by turning off the furnace power and the diffraction patterns were collected in non-isothermal conditions during cooling.

Contrary to the αMn phase that never reappears, the nitride is visible as disordered *fcc* in the pattern measured between 903°C and 877°C, then as the ordered $L1_2$ phase in the pattern measured between 682°C and 593°C. The temperatures are consistent with the heating cycle considering the non-equilibrium conditions. Lower amount of $L1_2$ and lower lattice parameter are explained by the loss of nitrogen that has occurred during heating.

The following process can therefore be anticipated. A nitride is initially present. It disorders at high temperature with an associated loss of nitrogen. At the σ/bcc phase transition, nitrogen partitions into the *bcc* phase in which it is probably more soluble than in the σ phase. The amount in the *fcc* phase decreases until there is no more nitrogen and the (not stable) *fcc* phase disappears completely. During cooling, *fcc* reappears at the same time as the σ phase to accommodate nitrogen that is not soluble in σ. The *fcc* phase transforms back into $L1_2$ but in lower amount and with a smaller lattice parameter because some nitrogen has been lost in the vacuum of the furnace.

The intensity problems encountered with the first sample were not found with this second sample because of lower maximum temperature and fast transformation from *bcc* to σ, so that the σ phase could be refined with Rietveld. However, due to the small acquisition time (1 min then 10 min), the diffraction patterns have not a sufficient quality to allow the refinement of site occupancies. These could be obtained only on the two last measurements of 30 min at the lowest temperatures (~200°C and 100°C).

4.3. $Cr_{34}Mn_{66}$

A sample was synthesized at the composition $Cr_{34}Mn_{66}$ in order to verify the existence of the α' phase. The results are presented in Table S1 of Supplementary Material. The sample was first annealed at 800°C during 3 weeks in the temperature range in which Wachtel and Bartelt reported this phase [8]. At this temperature, we observed equilibrium between the σ and the *bcc* phase. No evidence of any additional phase is observed. The lattice parameter of the *bcc* phase corresponds to the lattice parameters of the *bcc* solid solution as reported in Refs. [18, 19]. Since Pearson and Hume-Rothery [7] observed this phase at lower temperature than Wachtel and Bartelt (they draw a tentative peritectic decomposition at 600°C), other additional annealing treatments were conducted at lower temperatures (700°C and 550°C). Except slight modifications of the compositions related to changes of the solubilities as a function of temperature, no difference was observed as far as phase constitution is concerned. So, the existence of the α' phase can be excluded in our investigation.

5. Discussion

5.1. Equilibrium conditions

It can be questioned if equilibrium was reached at the different temperature steps. This is probably not the case during fast quenching. But, for the other isothermal measurements the reproducibility and coherency between results (between the two samples, between heating and cooling) seem to indicate that equilibrium has been reached. The σ to *bcc* transformation is congruent so there is no diffusion, and this is in favor of a rapid establishment of equilibrium. Patterns in which both *bcc* and σ are observed at the same time may be attributed either to the existence of a two phase domain in the phase diagram (mandatory if the sample has not the exact congruent composition) or to a small kinetic effect. The transformation of *bcc* into σ in cooling is so fast, as demonstrated by the quenching experiment, that it is sure that equilibrium is reached within the acquisition time of the patterns in isothermal conditions (30 min). For the σ/*bcc* transformation, a small hysteresis may be seen between heating and cooling. Even, the nitride precipitation (this time with diffusion) in sample $Cr_{23}Mn_{77}$ is well reproducible between heating and cooling. Only the nitrogen composition is modified due to the nitrogen loss under vacuum.

5.2. Lattice parameters

The increase of the lattice parameters of the σ phase as a function of temperature is nearly isotropic with a slight increase of *c/a* ratio of 0.4% between room temperature and 1000°C. It compares well with the previous results of Ref. [20]. The volume thermal expansion can be evaluated from Fig. 5 and is similar in the two samples.

The transformation to the *bcc* phase is associated with a significant (2.0 %) volume increase, probably related to the difference of compacity between the two structures (the average experimental compacity of the σ phase deduced from Ref. [1] is quite high: 74%). This value can also be compared to the volume change in iron at the *bcc*/*fcc* transition (-1.2 %) [21]. This difference explains the huge jump of the thermal expansion noticed in previous works [6, 9]. Larger volume of the *bcc* phase in sample $Cr_{23}Mn_{77}$ despite similar σ phase volume is attributed to the nitrogen solubility in this phase.

5.3. Displacement parameters

The displacement parameter typically increases with temperature for the σ phase from 0.5 $Å^2$ to ~1.5 $Å^2$ at the transition temperature (1000°C). Similar values are observed for the two samples. For the *bcc* phase, significantly higher values are measured from 2.5-3 $Å^2$ up to 3.5 $Å^2$ at 1200°C. The difference may be related to the smaller packing of this structure.

5.4. Analysis of site occupancies

The site occupancies in the σ phase have been refined as a function of temperature for the two samples. They are plotted in Fig. 6. As usual for the σ phase, a large amount of disorder is noticed even at room temperature. The two atoms mix in all sites showing only site preference. Cr, the atom with less electron, prefers the high CN sites (CN14 and 15) than the low CN sites (CN12). It is however important to note that CN15 is not the most occupied by Cr. Differences between the two samples are mostly related to the difference of composition. Therefore, Cr site occupancies in all sites are always larger for sample $Cr_{23}Mn_{77}$ (real composition $Cr_{28}Mn_{72}$) than for sample $Cr_{21}Mn_{79}$ (real composition $Cr_{22.5}Mn_{77.5}$).

Slight but visible changes of site occupancies as a function of temperature can be noticed. They are similar in the two samples. They correspond to an increase of the disorder *i.e.* a decrease (respectively increase) of the site occupancies when larger (respectively lower) than the composition.

Our previous results obtained at room temperature from alloys quenched from 900°C and 1050°C correspond more to the room temperature site occupancies than to the ones at the temperature of the annealing treatment. This means that the state of order in the σ phase cannot be quenched and that the observation of site occupancies do not correspond to the temperature of the preparation. This is why *in situ* measurements appears to be extremely useful. As far as we are aware, such measurement has never been reported previously on the σ phase in any other system.

Then, a comparison can be made with the site occupancies calculated using DFT and the Bragg-Williams approximation (for a complete description of the calculations, see *e.g.* Ref. [22]). Two datasets were obtained (spin-polarized and non spin-polarized). The calculation from the spin-polarized dataset gives the best agreement with the data. Qualitatively, the agreement is very good, but, quantitatively, not only the level of order at room temperature but also the variation of the level of order as a function of temperature is overestimated in the calculation. This could be interpreted as a sign that entropy contributions should be introduced (in our calculation, only enthalpies and ideal mixing on the different sites are considered).

5.5 High temperature σ phase transition

As reviewed in Section 2, there exist several indications that a transition occurs around 1000°C in the composition domain of the σ phase. Note that Zwicker [6] saw the transition but refrained from proposing an interpretation. Pearson and Hume-Rothery noticed that the high and low temperature σ phases had the same XRD structure [7]. This was checked by *in situ* XRD at high temperature. They did not specifically speak about an order-disorder transition, which was eventually done by Wachtel and Bartelt [8] because quenched alloys from the high and the low temperature fields were identical. In brief, there exist proofs that something is happening, but the proposal of the disorder is just an interpretation mainly based on the fact that alloys quenched from the high temperature present the same diffraction patterns. It was thought that it was corresponding to different states of order that cannot be seen from XRD. This proposal was retained in the evaluation of the system [2].

A careful reading of the literature could however have raised suspicions that this interpretation was not correct. For example, one should have noticed that alloys in the σ phase region become ductile above 1000°C and could easily be deformed [6]. A more important observation can be made. The σ phase is already disordered by nature. The already known measurements of site occupancies on this and other binary systems shows that all the sites are shared by the two atoms. Though there exists site preference, this is however not sufficient to imagine that it could further disorder, in particular in a first-order transition accompanied by a so large variation of the other properties (like volume for example). It is even more difficult to imagine how two order-disorder transitions could exist as reported by Wachtel and Bartelt [8].

Concerning this later work, several comments can be made. First, it is apparent, and even noticed by the authors, that the high temperature phase cannot be retained by quenching (it has the same measured magnetic susceptibility as the low temperature phase). Secondly, contrary to alloys annealed at temperature below 1000°C for which the susceptibility evolves linearly in the two-phase region between the susceptibilities corresponding to the two phases (see Fig. 4 in Ref. [8]), the alloys annealed at 1100°C present a strongly different behavior, noticed but not explained by the authors. For these alloys, the susceptibility suddenly drops to the value corresponding to that of the σ phase at Mn compositions above 70 at.% (Fig. 2 of their paper). This cannot be explained by the phase diagram reported by these authors. Finally, another feature that is not explained is the measurement they did *in situ* at 1150°C (Fig. 2 of their paper) that shows a constant variation of the susceptibility in agreement with a single phase domain at high temperature, unless one considers that the so-called disordered σ phase has the same susceptibility as the *bcc* phase.

It should already have been clear that the phase observed in quenched samples has been transformed into the low temperature phase and that it is not the high temperature phase. So, there was no reason to suppose that the high temperature phase had the same structure as the σ phase. A comparison with other systems like V–Mn, for example should have given the solution.

In present work, we clearly identified the nature of the phase transition observed in previous work as a congruent transformation of the σ phase into a *bcc* phase. It is not only evident from the *in situ* ND data but it also explains all the features of the previous literature: the thermal arrest, the ductility above 1000°C, the order of the transition, the discontinuity of the volume.

It also explains the susceptibility measurements: the same susceptibility of the high temperature phase when quenched, the continuous susceptibility when measured at 1150°C and the sudden drop as a function of composition of alloys quenched from the high temperature (if one considers that 70 at.% Mn is the upper limit above which the *bcc* solid solution can no longer be quenched from 1100°C, then above this composition, single phase σ phase is obtained – metastable between 70 at.% and 75 at.% Mn – explaining why two phase domain is not noticed in the susceptibility-composition curve).

Though we could not apply a very high cooling rate in the furnace, we could nevertheless reproduce the transformation during cooling to the σ and confirm that the *bcc* phase could not be quenched in accordance with the previous literature indicating the presence of the σ phase after quenching from the high temperature. It is well known, anyway, that *bcc* δMn can neither be retained by quenching, so the region of instability at low temperature starts at 70 at.% Mn and proceeds to pure Mn.

The only point that is not explained is the high temperature *in situ* XRD measurements by Pearson and Hume-Rothery [7]. Above 1000°C, they should have noticed the transformation into *bcc*. The only explanation is a wrong calibration of the temperature measurement in their experiment.

This congruent transformation is similar to what is present in many other systems: Cr–Fe, Co–Cr, Fe–V, Mn–V… Interestingly, in Mn–V system, Waterstrat mentioned that the *bcc* phase could be retained only on the outer portion of the samples after quenching while the inside had transformed to the σ phase [23]. One can note the very strong similarity between the Mn–V system and the revised Cr–Mn system proposed in this work.

It is also interesting to note that Gudzenko and Polesya [10, 11] observed the *bcc* phase in quenched alloys in the region of the σ phase when extremely high cooling rates are used (10^7-10^8 °C/s). They interpreted their experiment as the formation of a metastable phase during non-equilibrium cooling. On the contrary, they did observe the real high temperature equilibrium state with this odd technique while the conventional annealing-quenching technique failed.

Finally, this study cast doubts on all the other systems in which order-disorder transition in the σ phase has been reported (but never shown from a structural point of view): Cr–Co, Cr–Fe, V–Co, V–Fe, V–Ni. These systems have already been reviewed in Ref. [1]. Once again, one should carefully examine the evidence and perhaps check with *in situ* ND as an ultimate proof or disproof.

5.6 Low temperature σ phase transition

Our study shows also that the other transition proposed by Wachtel and Bartelt at 800°C [8] on the only basis of slight variations of the susceptibility (Fig. 7a of their paper) neither exists. Slight changes of the magnetic properties could perhaps explain the anomalies observed without having to introduce a structural modification, which is actually not shown by diffraction.

5.7 α’ phase

Pearson and Hume-Rothery were the first to notice the presence of the α' phase in alloys of composition close to $Cr_{40}Mn_{60}$ [7]. It was always found in three-phase alloys with *bcc* and σ phase which should have drawn attention. Moreover, the quantity of this new phase diminishes as a function of the annealing time between 800°C and 600°C. Only below 600°C, was thought the phase to be stable though equilibrium could never be obtained (three phases are always present) and though erratic results concerning the phase amount were obtained as a function of

either the annealing time or the nominal composition. The reason for the presence of the phase above 600°C was not explained. The structure was identified as αMn structure based on 11 indexed diffraction lines which also calls attention because this is the structure of pure Mn at these temperatures.

Wachtel and Bartelt also reported this α' phase [8]. It was revealed by a change of slope of the magnetic susceptibility-composition curves (Fig. 4 of their paper). According to their interpretation, it is formed by a peritectoid reaction at 925°C. The great discrepancy between this temperature and that reported by Pearson and Hume-Rothery (600°C) is not noticed by Wachtel and Bartelt. The equilibrium is never reached so that the phase could never be isolated. It could not be seen in the metallographic examination and the αMn crystal structure is hardly confirmed: only one diffraction peak is visible. A magnetic anomaly detected at 600°C is interpreted as an order-disorder transition.

On the other hand, the α' phase has not been detected by several other authors [6, 24] despite alloys prepared in the corresponding phase diagram region. These authors have not used annealing treatment at high temperature.

Carlile *et al.* [3, 14] and Zwicker [6] described the extreme sensitivity of the Cr–Mn alloys to nitrogen. Above 1050°C, silica tubes used to perform annealing treatments become permeable to nitrogen and alloys are rapidly contaminated. The contamination is seen by the presence of needle-shaped nitrides. Even Wachtel and Bartelt [8] confirmed this high sensitivity to nitrogen and does not exclude the presence of contamination in their samples. Pearson and Hume-Rothery [7], on the other hand, do not seem to have paid attention to nitrogen contamination and quartz tubes were used for homogenization treatments.

We claim that the so-called α' phase in the works of Pearson and Hume-Rothery [7] and Wachtel and Bartelt [8] is in fact a ternary nitride corresponding to the ternary extension of Mn_4N with Cr substitution. There is no doubt that the additional phase in our sample $Cr_{23}Mn_{77}$ is a nitride. The structure that could be refined from XRD and ND perfectly matches the structural model of Juza [15]. Though only semi-quantitative analysis could be performed, the presence of nitrogen in the order of 20 at.% could be shown by EDS. As shown in previous work, the contamination is probably due to the diffusion of nitrogen through the silica above 1100°C and the extreme sensitivity of these samples (related probably to the very high stability of this nitride and to the very small solubility in the σ phase). Sample $Cr_{34}Mn_{66}$ with a metallic composition closer to that of the nitride was not contaminated because it was never annealed at very high temperature. Sample $Cr_{21}Mn_{79}$ neither contained nitride. This composition is perhaps less sensitive or, maybe, there is a dependence on the quality of different silica batches. From the ternary phase diagram of the Cr–Mn–N system [16], the presence of αMn is very well understood. It is the product of decomposition of the σ phase into the nitride if the nitride has higher Cr content than the σ phase. There is indeed the presence of a three-phase equilibrium between σ, αMn (the manganese solid solution) and the nitride $(Mn,Cr)_4N$.

We believe that what we have observed corresponds to what was obtained in the previous literature and that the presence of the ternary nitride was mistakenly attributed to the presence of a new binary phase. The procedure adopted in the present work was similar to that used by other authors. The metallic ratio measured in our nitride perfectly matches the composition of the so-called α' phase. The indexing of this new phase with the αMn structure, instead of being a proof of its existence, is on the contrary a proof of the contamination since there is no reason why αMn should be restabilized in the binary system at this composition while it may appear in a ternary system. Finally, all the anomalies (always three phases, non reproducibility, erratic results, differences between authors) are well accounted for by non-reproducible nitrogen content. Even the anomaly at 925°C observed by Wachtel and Bartelt [8] is explained in our *in situ* experiment by the disordering of the filled $L1_2$ phase into *fcc* and the disappearance of αMn. Finally, the anomaly at 600°C could be attributed to the Curie temperature of this ferromagnetic compound. Last but not least, sample $Cr_{34}Mn_{66}$, in spite of very long annealing treatments, at different temperatures never showed other phases than σ and *bcc*.

The filled $L1_2$ structure proposed by Juza *et al.* [15] for the Cr substitutional derivative of Mn_4N could be confirmed. We found a significantly larger solubility limit for Cr (Cr/(Cr+Mn)=0.4 compared to 0.2) that may be explained by the different temperature of formation (1100°C compared to 750°C). This is also in contrast with the report of the ternary phase diagram by Ettmayer *et al.* [16] but as the nitrogen pressure is significantly different, this parameter may strongly affect the relative stabilities of the different nitrides.

What is completely new is the fact that the nitride is observed to disorder into *fcc* at a temperature situated probably around 700°C which could not be detected previously without the use of neutron diffraction.

This apparent disordering may also be seen as a change of phase equilibrium from σ + Mn_4N to σ + γMn (+ N_2), Mn_4N and γMn being the ordered and disordered variant of the same phase, though showing up as distinct in the phase diagram [25].

It can be seen from the phase diagram that this allotropic (*fcc*) form of Mn stable between 1100°C and 1138°C for the pure element is stabilized at lower temperature by Cr substitution. It is also stabilized in the binary Mn–N system [25]. The ternary extension may therefore be quite large as a function of composition and down to lower temperature.

Interestingly, according to our refinement of nitrogen content, the *fcc* phase is stable down to extremely low nitrogen concentration therefore very close to the binary border.

Contrary to the σ phase, the *bcc* phase appears to have a nitrogen solubility.

The refined nitrogen content should be taken with care. In the filled $L1_2$ phase, it does not match the expected quantity of about 1 N per cell corresponding to the composition Mn_4N and our semi-quantitative analysis of nitrogen content. However, the refined quantity strongly depends on the ordering model chosen for the metal atoms. In our model, we fixed Mn on site 1*a* and refined Cr substitution on site 3*c* but a different atom distribution would lead to a much different refined N content. For the same reason, the phase amount may be overestimated in ND experiment (~24 wt.% compared to 4 wt.% in XRD experiment). One should also not forget that this phase is always a secondary phase in our sample so that the refinement cannot be of the highest accuracy.

5.8 Updated phase diagram

We propose in Fig. 7 an updated version of the phase diagram. The new drawing involves the disappearance of several invariant points. Most reported high temperature reactions involving the σ phase were anticipated in the previous description because of their necessary presence rather than by the measurement of a thermal arrest. On the contrary Carlile *et al.* [3] mentioned that non definite arrests were obtained on cooling curves. The eutectic between σ and γ-Mn mentioned by Zwicker [4] (not confirmed in further work) could be a minimum of the liquidus corresponding to the congruent melting of *bcc* at this composition.

5.9 Thermodynamic modeling

The phase diagram was modeled by Lee [26] using the Calphad method. He considered both the presence of α' phase and the order-disorder transition in the σ phase with two separated phases in the modeling (the normal σ phase and a high temperature σ phase). Apparently, the system has not been reassessed apart from slight modifications [27]. Similar versions are also present in the commercial thermodynamic databases such as TCHEA4 and TCNI8 (CR3MN5 for α' and CRMN3_HT_SIGMA or HIGH_SIGMA for the σ phase above 1000°C) and TCFE9 (HIGH_SIGMA, the α' phase is not considered). Interestingly, suspending the CR5MN5 and HIGH_SIGMA in the calculations leads to an approximately correct phase diagram. In particular, the continuous *bcc* solid solution is calculated. However, modifications should be made to the homogeneity domain of the σ phase in particular at low temperature. All the calculated ternary systems based on Cr–Mn system should also be checked carefully.

6. Conclusions

We used *in situ* powder ND to characterize two regions of the Cr–Mn phase diagram. In contrast with the literature, no order-disorder transition for the σ phase at high temperature can be seen. Instead, a congruent transformation to the disordered *bcc* phase is established. The other transformation in the σ phase at lower temperature reported by one author [8] neither exists. The other reported intermetallic phase of this system (the so-called α' phase) does not exist and is shown to be a ternary nitride. An updated phase diagram is therefore proposed.

More general conclusions concerning determination and evaluation of phase diagrams can be drawn. Even in very common (and important) systems that are thought to be well known, important errors may still be found. Most of these systems have been characterized and fixed in the literature in the 50's or 60's. Though the studies were conducted very carefully, the analytical techniques were not as sensitive as nowadays. No elemental analysis was existing and techniques such as powder XRD were extremely limited (film measurements) compared with what can be done now with a numerical treatment of a powder pattern obtained on a diffractometer (better resolution, indexing databases...). Details like slight changes of lattice parameters, careful indexation, observation of minority phases could not be seen. This severely limited the precision and the reliability of the determination.

It is noteworthy that for many systems, like Cr–Mn studied in this article, no investigation has been conducted since then, and a verification with newer analytical techniques is missing. It is also striking as wrong hypothesis, based on limited evidence, can propagate in the literature, and be accepted without questioning. In the case of Cr–Mn, not even speaking about the use of ND, and as shown in the discussion, a careful study of the literature on this and other related systems should have been sufficient to identify that there were problems, that the hypothesis of an order-disorder transition did not make sense and that the existence of the α' phase was questionable.

As a rule, one should always be careful with phases that have not been identified from the structural point of view with a definite crystal structure. The lack of an identified crystal structure for both high temperature σ and, to a certain extent, for α' should have been taken as an indication. Another conclusion is that phase diagrams cannot be drawn on the only basis of indirect measurements like susceptibility or thermal expansion since there is a high risk of misidentification of the transformations when these measurements are not supported by structural data. This should be better taken into account by evaluators of phase diagrams.

Acknowledgements
The following persons are deeply acknowledged: Jean-Claude Crivello for the DFT calculations, Qing Chen from Thermo-Calc company for discussion, Rémi Pires and Yvan Cotrebil for the preparation and the EBSD measurements, Diane Muller for the EDS measurement, Eric Leroy for the EPMA measurements, Valérie Lalanne for the preparation of the samples.

Figures:

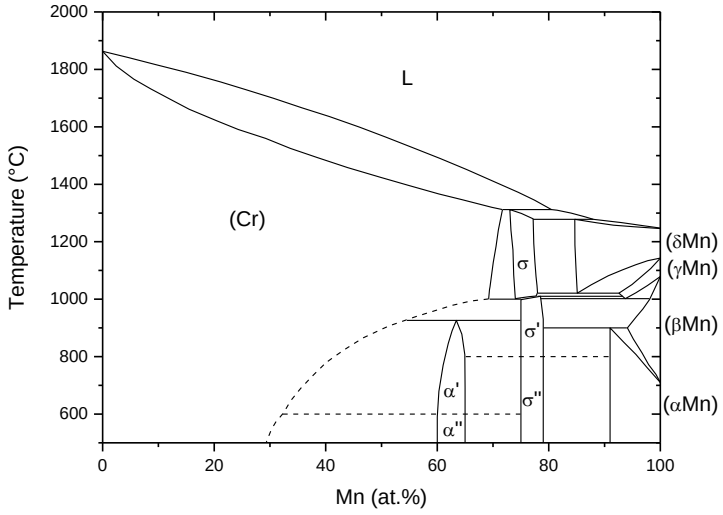

Figure 1: phase diagram of the Cr–Mn system from the literature (redrawn from Ref. [2]).

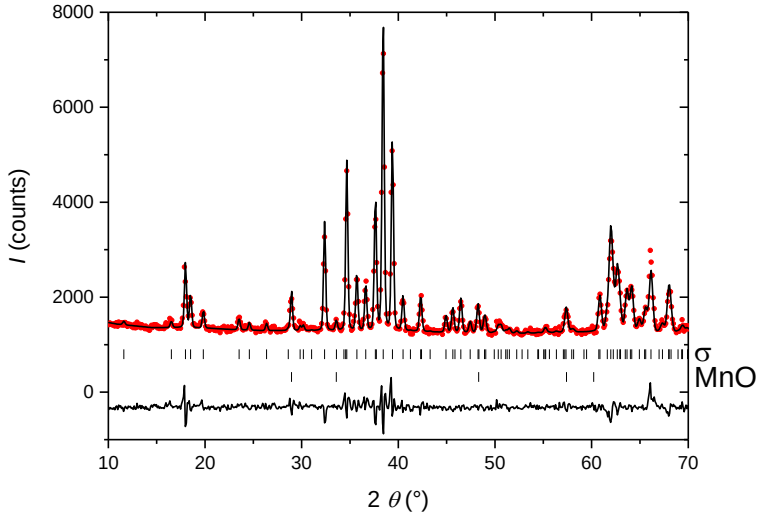

Figure 2: Rietveld plot of the ND pattern of sample $Cr_{21}Mn_{79}$ at room temperature before the experiment in a vanadium container (only a limited range is shown). Experimental (points), calculated (line) and difference (line below) patterns are shown. The markers show the positions of the diffraction lines of the σ phase and MnO.

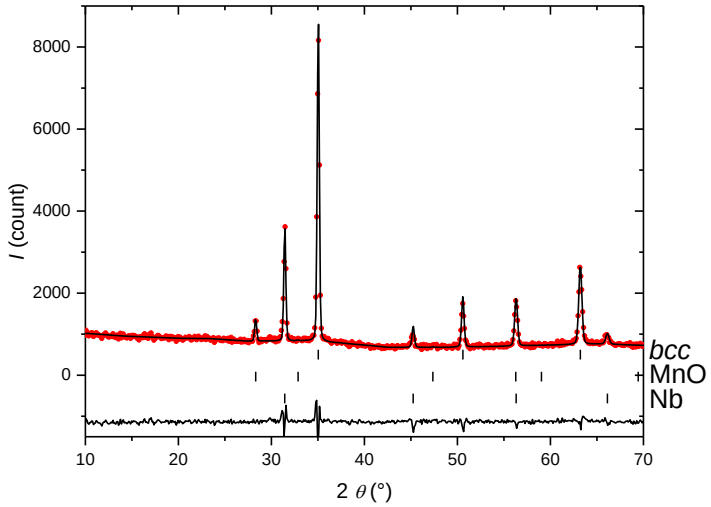

Figure 3: Rietveld plot of the ND pattern of sample $Cr_{21}Mn_{79}$ at 1050° (first heating) (only a limited range is shown). Experimental (points), calculated (line) and difference (line below) patterns are shown. The markers show the positions of the diffraction lines of the *bcc* phase, MnO and the Nb container.

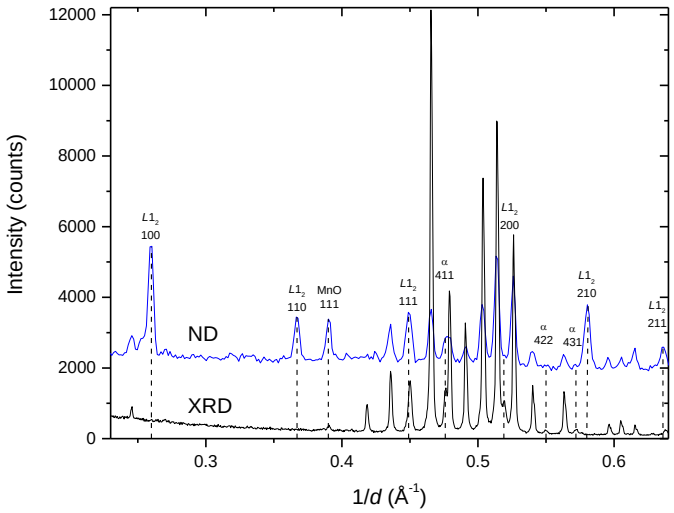

Figure 4: XRD (black) and ND (blue) patterns of $Cr_{23}Mn_{77}$ sample at room temperature with indexation of the supplementary phases. Non indexed lines correspond to the σ phase.

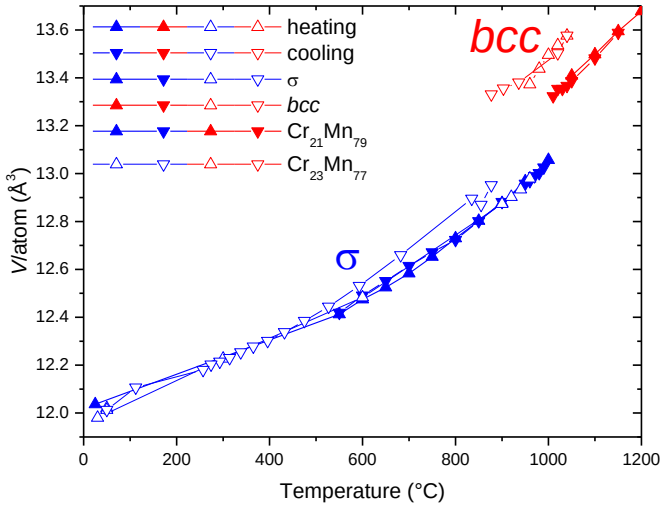

Figure 5: atomic volume of the σ and *bcc* phases as a function of temperature for the two samples $Cr_{21}Mn_{79}$ and $Cr_{23}Mn_{77}$.

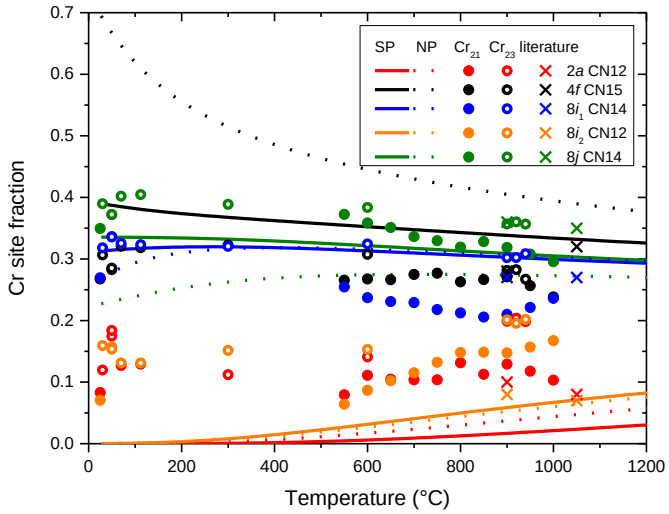

Figure 6: site occupancies in the σ phase. Experimental data for the two sample $Cr_{21}Mn_{79}$ and $Cr_{23}Mn_{77}$ are presented together with *ex situ* data from the literature [1]. Estimated standard deviations are between 1 and 2% depending on the site. Calculated data from DFT (spin-polarized and non spin-polarized) and Bragg-Williams approximation are also shown.

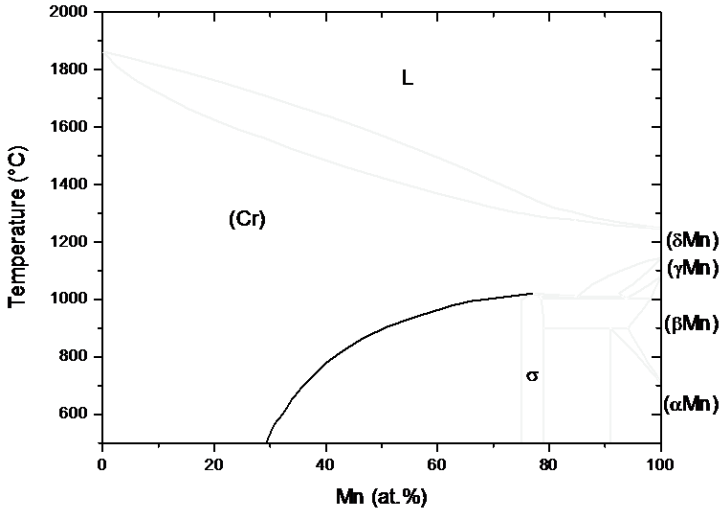

Figure 7: revised Cr–Mn phase diagram according to the present work.

References

[1] J.-M. Joubert, Crystal chemistry and Calphad modelling of the σ phase, Prog. Mater. Sci. 53 (2008) 528-583. https://doi.org/10.1016/j.pmatsci.2007.04.001.

[2] M. Venkatraman, J.P. Neumann, The Cr-Mn (chromium-manganese) system, Bull. Alloy Phase Diagr. 7 (5) (1986) 457-462. https://doi.org/10.1007/BF02867810.

[3] S.J. Carlile, J.W. Christian, W. Hume-Rothery, The equilibrium diagram of the system chromium-manganese, J. Inst. Met. 76 (1949) 169-194.

[4] U. Zwicker, Das System Mangan-Chrom, Z. Metallkd. 40 (10) (1949) 377-378. https://doi.org/10.1515/ijmr-1949-401005.

[5] W.B. Pearson, J.W. Christian, W. Hume-Rothery, New sigma-phases in binary alloys of the transition elements of the first long period, Nature 167 (January 20) (1951) 110. https://doi.org/10.1038/167110a0.

[6] U. Zwicker, Über eine Umwandlung der Phase Mn_3Cr im System Mangan-Chrom, Z. Metallkd. 42 (9) (1951) 277-278. https://doi.org/10.1515/ijmr-1951-420905.

[7] W.B. Pearson, W. Hume-Rothery, The constitution of chromium-manganese alloys below 1000°C, J. Inst. Met. 81 (1952-53) 311-314.

[8] E. Wachtel, C. Bartelt, Suszeptibilitätsmessungen im System Chrom-Mangan, Z. Metallkd. 55 (1) (1964) 29-36. https://doi.org/10.1515/ijmr-1964-550104.

[9] M. Gerspacher, Contributions à l'étude des transformations ordre-désordre dans les phases sigma. Précisions sur le diagramme Nickel-Vanadium, Thèse de Docteur-Ingénieur, Faculté des Sciences de Strasbourg, France (1970).

[10] V.N. Gudzenko, A.F. Polesya, Peculiarities of the rapid crystallization of binary alloys (of transition metals) in the concentration region of the existence of the σ-phase, Soviet Non-Ferrous Metals Research 17 (6) (1974) 353-356.

[11] V.N. Gudzenko, A.F. Polesya, Metastable phases in manganese based alloys, Russ. Metall. (5) (1975) 153-156.
[12] S.H. Algie, E.O. Hall, Site ordering in some σ phase structures, Acta Crystallogr. 20 (1966) 142. https://doi.org/10.1107/S0365110X66000276.
[13] J.S. Kasper, R.M. Waterstrat, Ordering of atoms in the σ phase, Acta Crystallogr. 9 (1956) 289-295. https://doi.org/10.1107/S0365110X56000802.
[14] S.J. Carlile, W. Hume-Rothery, A note on the effect of nitrogen on the structures of certain alloys of chromium and manganese, and on the existence of an intermediate nitride phase, J. Inst. Met. 76 (1949) 195-200.
[15] R. Juza, K. Deneke, H. Puff, Ferrimagnetismus des Mischkristalle von Mn_4N mit Chrom, Eisen und Nickel, Zeitschrift für Elektrochemie 63 (5) (1959) 551-557. https://doi.org/10.1002/BBPC.19590630503.
[16] P. Ettmayer, A. Vendl, E. Horvath, R. Kieffer, Beitrag zur Kenntnis des systems Chrom-Mangan-Stickstoff, Monatsh. Chem. 109 (1978) 1277-1285. https://doi.org/10.1007/BF00906039.
[17] J.-M. Joubert, R. Cerný, M. Latroche, A. Percheron-Guégan, K. Yvon, Site occupancies in $LaNi_5$ three-substituted compound determined by means of multiwavelength X-ray powder diffraction, J. Appl. Crystallogr. 31 (1998) 327-332. http://dx.doi.org/10.1107/S0021889897010911.
[18] S. Maki, K. Adachi, Antiferromagnetism and weak ferromagnetism of disordered bcc Cr-Mn alloys, J. Phys. Soc. Jpn. 46 (4) (1979) 1131-1137. https://doi.org/10.1143/JPSJ.46.1131.
[19] M. Shiga, M. Miyake, Y. Nakamura, Giant negative thermal expansion in Mn-rich bcc Cr-Mn alloys, J. Phys. Soc. Jpn. 55 (7) (1986) 2290-2295. https://doi.org/10.1143/JPSJ.55.2290.
[20] E. Lugscheider, P. Ettmayer, Hochtemperatur-röntgenographische Untersuchungen an manganreichen Mangan-Vanadin- und Mangan-Chrom-Legierungen, Monatsh. Chem. 102 (1971) 1234-1244. http://dx.doi.org/10.1007/BF00917177.
[21] X.-G. Lu, M. Selleby, B. Sundman, Assesments of molar volume and thermal expansion for selected bcc, fcc and hcp metallic elements, Comput. Coupling Phase Diagr. Thermochem. 29 (2005) 68-89. https://doi.org/10.1016/j.calphad.2005.05.001.
[22] K. Yaqoob, J.-C. Crivello, J.-M. Joubert, Comparison of the site occupancies determined by combined Rietveld refinement and by DFT calculations: the example of the ternary Mo-Ni-Re σ phase, Inorg. Chem. 51 (5) (2012) 3071-3078. https://doi.org/10.1021/ic202479y.
[23] R.M. Waterstrat, Investigation of the vanadium-manganese alloy system, Trans. AIME 224 (1962) 240-243.
[24] G.M. Lukashenko, V.R. Sidorko, Thermodynamic properties of Cr-Mn alloys, Russ. Metall. (1) (1989) 26-29.
[25] N.A. Gokcen, The Mn-N (manganese-nitrogen) system, Bull. Alloy Phase Diagr. 11 (1) (1990) 33-42. http://dx.doi.org/10.1007/BF02841582.
[26] B.-J. Lee, A thermodynamic evaluation of the Cr-Mn and Fe-Cr-Mn systems, Metall. Trans. 24A (1993) 1919-1933. http://dx.doi.org/10.1007/BF02666327.
[27] A. Jacob, E. Povoden-Karadeniz, Predictive computations of intermetallic σ phase evolution in duplex steel. I) Thermodynamic modeling of σ phase in the Fe-Cr-Mn-Mo-Ni system, Calphad: Comput. Coupling Phase Diagrams Thermochem. 71 (2020) 101998. https://doi.org/10.1016/j.calphad.2020.101998.